



Molecular Crystals and Liquid Crystals

Publication details, including instructions for authors and subscription information:

<http://www.tandfonline.com/loi/gmcl20>

Synthesis, Thermal and Luminescence Properties of Ortho-Terphenyl Derivatives with 1,3,4-Oxadiazole Moiety

E-Joon Choi ^a, Jun-Ha Hwang ^a, Eun-Kyoung Kwon ^a, Jung-Il Jin ^b, Yong-Hwan Ahn ^c, Young-Chul Kim ^c, Jae-Woong Yu ^d, Wen Sheng Shi ^e & Edward T. Samulski ^e

^a Department of Polymer Science and Engineering, Kumoh National Institute of Technology, Gumi, Gyungbuk, 730-701, Korea

^b Department of Chemistry, Korea University, Seoul, 136-713, Korea

^c Department of Chemical Engineering, Kyung Hee University, Yongin, Gyeonggi-do, 446-701, Korea

^d Center for Energy Materials Research, Korea Institute of Science and Technology, Seoul, 136-791, Korea

^e Department of Chemistry, University of North Carolina at Chapel Hill, Chapel Hill, North Carolina, 27599-3290, USA

Version of record first published: 18 Oct 2011

To cite this article: E-Joon Choi, Jun-Ha Hwang, Eun-Kyoung Kwon, Jung-Il Jin, Yong-Hwan Ahn, Young-Chul Kim, Jae-Woong Yu, Wen Sheng Shi & Edward T. Samulski (2011): Synthesis, Thermal and Luminescence Properties of Ortho-Terphenyl Derivatives with 1,3,4-Oxadiazole Moiety, Molecular Crystals and Liquid Crystals, 550:1, 189-204

To link to this article: <http://dx.doi.org/10.1080/15421406.2011.599740>

PLEASE SCROLL DOWN FOR ARTICLE

Full terms and conditions of use: <http://www.tandfonline.com/page/terms-and-conditions>

This article may be used for research, teaching, and private study purposes. Any substantial or systematic reproduction, redistribution, reselling, loan, sub-licensing, systematic supply, or distribution in any form to anyone is expressly forbidden.

The publisher does not give any warranty express or implied or make any representation that the contents will be complete or accurate or up to date. The accuracy of any instructions, formulae, and drug doses should be independently verified with primary sources. The publisher shall not be liable for any loss, actions, claims, proceedings,

demand, or costs or damages whatsoever or howsoever caused arising directly or indirectly in connection with or arising out of the use of this material.

Synthesis, Thermal and Luminescence Properties of Ortho-Terphenyl Derivatives with 1,3,4-Oxadiazole Moiety

E-JOON CHOI,^{1,*} JUN-HA HWANG,¹ EUN-KYOUNG KWON,¹
JUNG-IL JIN,² YONG-HWAN AHN,³ YOUNG-CHUL KIM,³
JAE-WOONG YU,⁴ WEN SHENG SHI,⁵
AND EDWARD T. SAMULSKI^{5,*}

¹Department of Polymer Science and Engineering, Kumoh National Institute of Technology, Gumi, Gyungbuk 730-701, Korea

²Department of Chemistry, Korea University, Seoul 136-713, Korea

³Department of Chemical Engineering, Kyung Hee University, Yongin, Gyeonggi-do 446-701, Korea

⁴Center for Energy Materials Research, Korea Institute of Science and Technology, Seoul 136-791, Korea

⁵Department of Chemistry, University of North Carolina at Chapel Hill, Chapel Hill, North Carolina 27599-3290, USA

A series of compounds and two polymers, all consisting of o-terphenyl and 1,3,4-oxadiazole units, were synthesized. They were characterized by GC, FT/IR, NMR, elemental analysis, viscometry, DSC, POM, TGA, and absorption and emission spectrometry. In general, by introducing an o-phenyl central core to 2,5-diphenyl-1,3,4-oxadiazole backbone, the processability of these materials was improved while maintaining a blue-light-emitting capability. The CIE coordinates of compounds with p-chloro, methoxy and t-butyl groups in EL devices were found to be (0.19, 0.16), (0.17, 0.13) and (0.18, 0.13), respectively, i.e., in the deep-blue region. Also, amorphous polymer with a m-phenylene unit, which shows good solubility in common organic solvents and excellent thermal stability, emits indigo-light at 415 nm on photoexcitation.

Keywords blue-light-emitting materials; amorphous and soluble OLED; thermally stable PLED; o-terphenyl derivatives; heteroaromatic moiety

1. Introduction

Organic luminescent materials have attracted much attention due to their potential application in a wide range of electronic and optoelectronic devices [1–3]. The full color display system requires three basic color materials for red, green, and blue emission [4–6]. A great number of red, green, and blue emitting materials have been synthesized and the details of structure-property relationships have been investigated [7]. However, pure blue light

*Corresponding author. E-mail: ejchoi@kumoh.ac.kr (E-J. Choi), et@unc.edu (E. T. Samulski)

emitting materials are still being sought after because of issues of color purity, thermal stability and fabrication problems. Recently reported blue emitting materials possess unique molecular geometries such as heterocyclic [8,9], non-coplanar [10,11], branched [12,13], and starburst [14–16] structures.

Aromatic polyoxadiazoles have excellent thermal and hydrolytic stability and fluoresce in the blue-greenish range, but their application is rather limited due to poor solubility in common organic solvents [17,18]. Although 1,3,4-oxadiazoles facilitate electron transport and hole blocking [19,20] via the electron-withdrawing character of the 1,3,4-oxadiazole ring, certain low molecular weight aromatic 1,3,4-derivatives have been used as blue emitters. However, the applicability of the oxadiazole moiety is limited because these materials have a short lifetime, possibly as a result of crystallization or aggregation effects. To overcome this problem, a variety of branched compounds, starburst structures, and small dendrimers have been advanced [21–24]. These materials are amorphous and form stable glasses, which minimizes the problems of crystallization. However, some attempts to improve solubility of these materials occasionally interrupted the conjugation of the main chain.

The principal purpose of our work was to improve the processability of conjugated materials while maintaining the blue-light-emitting properties. For this reason, we have synthesized a series of *o*-terphenylene derivatives with 1,3,4-oxadiazole moiety as blue-light-emitting materials and two polymers based on corresponding model compounds. The thermal, UV-Vis absorption, and photo- and electroluminescence properties of these materials were characterized and the findings are reported herein.

2. Experimental Section

2.1. Chemicals

N,N'-Diphenyl-*N,N'*-bis(1-naphthyl)-(1,1'-biphenyl)-4,4'-diamine (α -NPB) and tris(8-hydroxyquinoline) aluminium (Alq₃) were purchased from Gracel Company; terephthaloyl and isophthaloyl dihydrazides were purchased from TCI Company; 4-methoxybenzhydrazide was purchased from Lancaster Company. Solvents such as carbon disulfide, acetonitrile, phosphorus oxychloride and pyridine were purchased from Aldrich Company. The other reactants were purchased from Aldrich Company and the solvents from Fisher Company. 1,3,5-Tris(*N*-phenylbenzimidazol-2-yl)benzene (TPBI) was synthesized according to the reported procedures [25]; all the commercial reagents were used without further purification. Solvents such as thionyl chloride, dichloromethane and *N,N*-dimethylacetamide were purified by standard methods; the other solvents were used without further purification.

2.2. Instrumentation

NMR spectra of compounds **4a–4c** and **4d–7b** were recorded by a Bruker Advance 400 MHz and a Bruker DMX 200 MHz NMR spectrometer, respectively. IR spectra were obtained using a Jasco 300E FT/IR spectrometer. To confirm the degree of purity of compounds **4a–4c**, a GC was performed using a Hewlett Packard 5890 Series II gas chromatograph and for compounds **4d–7b**, elemental analyses were performed using a Thermofinnigan EA 1108 elemental analyzer. The phase transition temperatures were determined by a differential scanning calorimeter (Seiko DSC 220C for compounds **4a–4c**; DuPont

TA910 DSC for compounds **4d–7b**) and a polarizing optical microscope (POM: Nikon Microphot-FX for compounds **4a–4c**; Zeiss, Jenapol for compounds **4d–7b**) equipped with a hot stage (Linkam TMS 600 for compounds **4a–4c**; Mettler FP82HT for compounds **4d–7b**). DSC measurements were performed in a N₂ atmosphere with heating and cooling rates of 10°C/min. Thermal stability of polymers was measured using a DuPont TGA 2950 in a N₂ atmosphere with a heating rate of 20°C/min. Solution viscosities of obtained polymers were measured at 30°C using a Ubbelohde-type viscometer. UV-visible spectra were recorded using a Perkin Elmer Lambda 40 spectrometer for compounds **4a–4c**, a Scinco S-1100 spectrometer for compounds **4d–4g**, and a Hewlett-Packard 8452A spectrometer for polymers **7a** and **7b**. PL spectra were obtained by using a Spex 1403.35m double spectrometer with a PTI xenon arc lamp and PMT detector for compounds **4a–4c**, a Perkin Elmer LS 50 spectrometer for compounds **4d–4g**, and an Aminco Bowman Series 2 spectrometer for polymers **7a** and **7b**. The absorption and emission spectra were measured in diluted CHCl₃ solutions with concentrations of about 1.0×10^{-5} mol/L and 1.0×10^{-4} mol/L, respectively, at room temperature. Electroluminescence (EL) spectra of the EL devices were measured with a JBS IVL-300 EL characterization system in an ambient atmosphere.

2.3. Syntheses of bis(5-phenyl-1,3,4-oxadiazole-2-diyl) 4,4'-o-terphenyl (4a), bis(5-(o-chlorophenyl)-1,3,4-oxadiazole-2-diyl) 4,4'-o-terphenyl (4b), and bis(5-(p-chlorophenyl)-1,3,4-oxadiazole-2-diyl) 4,4'-o-terphenyl (4c)

The syntheses of compounds **4a–4c** were carried out as previously reported [26].

2.4. Synthesis of bis(5-(p-methylphenyl)-1,3,4-oxadiazole-2-diyl) 4,4'-o-terphenyl (4d)

o-Terphenyldicarboxylic acid (0.50 g, 1.57 mmol) was refluxed in 25 mL of SOCl₂ for 4 h. Excess SOCl₂ was removed by distillation under reduced pressure. The prepared 4,4'-*o*-terphenyldicarbonyl dichloride (**1**) was dissolved in 20 mL of methylene chloride. To this solution was added slowly a solution of *p*-toluic hydrazide (**2d**) (0.43 g, 3.14 mmol) dissolved in 10 mL of pyridine (2:1 v/v) at room temperature under a dry N₂-gas atmosphere, while stirring vigorously. After stirring at 90°C for 16 h, the mixture was concentrated by evaporating the solvent under reduced pressure. The residue was cooled to room temperature and poured into 250 mL of water. The resulting precipitate was collected by filtration, thoroughly washed with water and dried under vacuum at 60°C. The obtained intermediate (**3d**) was used for the next synthetic step without further purification. The dihydrazide **3d** was then added to a mixture of phosphoryl chloride (10 mL) and acetonitrile (30 mL). The reaction mixture was heated at 100°C for 16 h, and then it was concentrated by evaporating the solvent under reduced pressure. The residue was cooled to room temperature and carefully submersed in 200 mL of ice-water to hydrolyze the residual POCl₃. The resulting solid was washed thoroughly with water, collected by filtration, dried under vacuum at 60°C, and purified by using a column chromatography on silica gel with a mixture of hexane and ethyl acetate (1:2 v/v). Further purification was conducted by re-precipitation: dissolved in chloroform, filtered by a PTFE membrane filter, crystallized from hexane, and dried under vacuum at 60°C. Yield: 87%; TLC (silica gel, hexane/ethyl acetate = 1:2, v/v), R_f 0.97. IR (KBr Pellet, cm⁻¹): 3043 (aromatic =C-H, st), 1613, 1576 (aromatic C=C, st), 1265, 1181, 1067 (C-O, st). ¹H NMR (CDCl₃, δ in ppm): 8.10–7.97 (8H, d, Ar-H), 7.56–7.51 (4H, s, Ar-H), 7.39–7.30 (8H, d, Ar-H). Elemental anal. Calcd for C₃₆H₂₆N₄O₂: C, 79.12; H, 4.76; N, 10.26. Found: C, 78.06; H, 5.39; N, 10.89.

2.5. Synthesis of bis(5-(*p*-methoxyphenyl)-1,3,4-oxadiazole-2-diyl) 4,4''-*o*-terphenyl (**4e**)

Compound **4e** was synthesized similarly to the compound **4d**. Yield: 72%; TLC (silica gel, hexane/ethyl acetate = 1:2, v/v), R_f 0.88. IR (KBr Pellet, cm^{-1}): 3012 (aromatic =C-H, st), 1611, 1496 (aromatic C=C, st), 1299, 1255, 1171, 1023 (C-O, st). ^1H NMR (CDCl_3 , δ in ppm): 8.10–7.96 (8H, d, Ar-H), 7.53–7.48 (4H, s, Ar-H), 7.07–6.96 (8H, d, Ar-H). Elemental anal. Calcd for $\text{C}_{36}\text{H}_{26}\text{N}_4\text{O}_4$: C, 74.74; H, 4.50; N, 9.69. Found: C, 69.49; H, 4.98; N, 9.84.

2.6. Synthesis of bis(5-(*p*-butyloxyphenyl)-1,3,4-oxadiazole-2-diyl) 4,4''-*o*-terphenyl (**4f**)

Compound **4f** was synthesized similarly to the compound **4d**. Yield: 88%; TLC (silica gel, hexane/ethyl acetate = 1:2, v/v), R_f 0.97. IR (KBr Pellet, cm^{-1}): 3050 (aromatic =C-H, st), 1611, 1555, 1523 (aromatic C=C, st), 1299, 1256, 1170, 1023 (C-O, st). ^1H NMR (CDCl_3 , δ in ppm): 8.10–7.96 (8H, d, Ar-H), 7.53–7.48 (4H, s, Ar-H), 7.07–6.96 (8H, d, Ar-H). Elemental anal. Calcd for $\text{C}_{36}\text{H}_{26}\text{N}_4\text{O}_4$: C, 74.74; H, 4.50; N, 9.69. Found: C, 69.49; H, 4.98; N, 9.84.

2.7. Synthesis of bis(5-(*p*-nitrophenyl)-1,3,4-oxadiazole-2-diyl) 4,4''-*o*-terphenyl (**4g**)

Compound **4g** was synthesized similarly to the compound **4d**. Yield: 89%; TLC (silica gel, hexane/ethyl acetate = 1:2, v/v), R_f 0.98. IR (KBr Pellet, cm^{-1}): 3042 (aromatic =C-H, st), 29.43 (C-H, st), 1612, 1556 (aromatic C=C, st), 1211, 1076 (C-O, st). ^1H NMR (CDCl_3 , δ in ppm): 8.11–7.98 (8H, d, Ar-H), 7.58–7.49 (4H, s, Ar-H), 7.39–7.31 (8H, d, Ar-H). Elemental anal. Calcd for $\text{C}_{42}\text{H}_{38}\text{N}_4\text{O}_2$: C, 80.00; H, 6.03; N, 8.89. Found: C, 78.72; H, 6.16; N, 8.92.

2.8. Synthesis of Poly(1,3,4-oxadiazole-2,5-diyl-4,4''-*o*-terphenyl-1,3,4-oxadiazole-2,5-diyl-*m*-phenylene) (**7a**)

Diacid dichloride (**1**) (1.57 mmol) was dissolved in 10 mL of *N,N*-dimethylacetamide (DMAc) in a nitrogen atmosphere. To this solution was added a solution of isophthalic dihydrazide (**5**) (0.30 g, 1.57 mmol) dissolved in DMAc (20 mL) by use of a syringe at room temperature, resulting in the production of hydrochloric acid gas. After agitation at 120°C for 16 hr, the reaction mixture was cooled to room temperature and poured into methanol (250 mL) to produce a precipitate. The resulting solid of precursor (**6a**) was filtered, washed several times with water and methanol, and dried under vacuum at 60°C to use in the next synthetic step. IR (KBr Pellet, cm^{-1}): 3470 (N-H, st), 3043 (aromatic =C-H, st), 1645 (C=O, st), 1528, 1474 (aromatic C=C, st), 1266 (C-N, st).

The poly(hydrazide) **6a** was added to a mixture of acetonitrile (30 mL) and phosphorus oxychloride (10 mL). After refluxing with vigorous stirring at 90°C for 16 hr, the mixture was cooled to room temperature and excess acetonitrile was removed at 50°C in a vacuum. Trace amounts of POCl_3 was hydrolyzed by adding ice water, and then precipitated in methanol. The resulting solid product was filtered, washed several times with water and methanol, and dried in a vacuum at 60°C. Yield: 70%. IR (KBr Pellet, cm^{-1}): 3053 (aromatic =C-H, st), 1612, 1545, 1471 (aromatic C=C, st), 1249, 1183 (C-O, st), 1073 (=C-O-C= ,

st). Elemental anal. Calcd for $C_{28}H_{16}N_4O_2$: C, 76.36; H, 3.64; N 12.73. Found: C, 71.27; H, 3.90; N, 12.29.

2.9. Synthesis of Poly(1,3,4-oxadiazole-2,5-diyl-4,4'-o-terphenyl-1,3,4-oxadiazole-2,5-diyl-p-phenylene) (7b)

Precursor **6b** was synthesized using the same method as precursor **6a** except a mixture of LiCl (5 wt%) and DMAc (30 ml) was used as a polymerization solvent. IR (KBr Pellet, cm^{-1}): 3477 (N-H, st), 3039 (aromatic =C-H, st), 1650 (C=O, st), 1533, 1473 (aromatic C=C, st), 1272 (C-N, st).

Polymer **7a** was synthesized using the same method as polymer **7b**. Yield: 76%. IR (KBr Pellet, cm^{-1}): 3053 (aromatic =C-H, st), 1612, 1570, 1499, 1474 (aromatic C=C, st), 1274, 1186 (C-O, st), 1073 (=C-O-C=, st). Elemental anal. Calcd for $C_{28}H_{16}N_4O_2$: C, 76.36; H, 3.64; N, 12.73. Found: C, 70.48; H, 4.12; N, 11.81.

2.10. Device Preparation

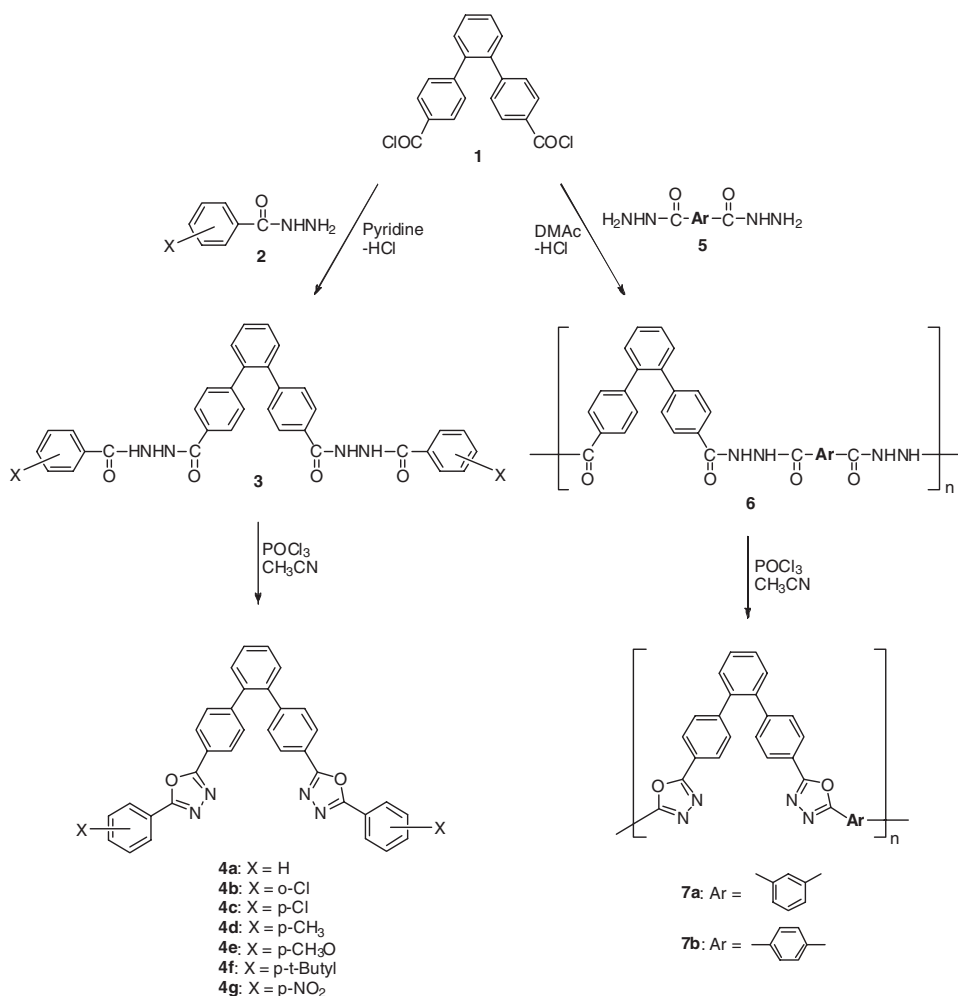
EL devices with the configuration of [ITO/ α -NPB(40 nm)/compounds **4c**, **4e** and **4f**(30 nm)/TPBI(10 nm)/Alq₃(30 nm)/LiF(1 nm)/Al(100 nm)] were prepared. For the devices, α -NPB was used as the hole transport layer (HTL), and TPBI and Alq₃ were used as the electron transport layer (ETL). Indium tin oxide (ITO) coated glass substrates (Asahi Glass Co., Ltd.) with a surface resistance of 10 Ω /sq were patterned by using a standard photolithography method and then cleaned by sonication in trichloroethylene, acetone, deionized water, and isopropyl alcohol. Thermal evaporation of organic materials and metals was carried out in a high vacuum condition (2×10^{-6} Torr) and the deposition rates were 1.0, 0.1, and 5–6 $\text{\AA}/s$ for the organic layer, the LiF layer, and the Al cathode, respectively. The deposition rate and thickness of each layer was regulated using a calibrated quartz crystal microbalance. The active emitting area of the device was $3 \times 3 \text{ mm}^2$.

Also EL devices with the configurations of [ITO(15 Ω)/CuPC(30 nm)/compounds **4d**, **4e** and **4f**(80 nm)/LiF:Al(100 nm)] and [ITO(15 Ω)/PEDOT(30 nm)/polymer **7a**(80 nm)/LiF:Al(100 nm)] were prepared. In the devices, copper phthalocyanine (CuPC) and poly(3,4-ethylenedioxythiophene-2,5-diyl) (PEDOT) were used as the hole transport (HTL) and the injection layer (HIL) for the compounds and the polymer, respectively. Deposition rate of compounds **4d** and **4e** was 0.5–6.0 $\text{\AA}/s$ at 77–78°C, and that of compound **4f** was 1.0–4.4 $\text{\AA}/s$ at 117–169°C. Thin film of polymer **7a** was obtained by spin-coating: the solution (40 μ l) of the polymer (40 mg) in TCE (1 mL) was spin-coated and then vacuum-dried at 150°C for 2 h. Obtained films were used to measure the absorption and emission spectra. PEDOT was spin-coated onto the polymer layer and dried at 100°C for 2 h.

3. Results and Discussion

3.1. Synthesis and Thermal Properties

The synthetic route to compounds and polymers is shown in Scheme 1: the 1,3,4-oxadiazoles (**4** or **7**) were prepared by cyclodehydration of the hydrazide precursors (**3** or **6**) which were obtained by reaction of 4,4'-o-terphenyldicarbonyl dichloride (**1**) and benzhydrazide (**2** or **5**). The structures of all compounds were identified using IR and NMR spectrometry. All of the resultant spectra were in accordance with expected values. The purities of compounds **4a–4c** reported by us [26] were confirmed by using TLC and GC methods. As a result, they



Scheme 1. Synthetic route to compounds and polymers.

showed a single R_f value in TLC plate as well as a sharp peak with a single elution time in GC chromatographs. The purities of compounds **4d–4g** and polymers **7a** and **7b** were confirmed by using an elemental analysis, and the data was within tolerable uncertainties.

Representative differential scanning calorimetric (DSC) thermograms are presented in Fig. 1, and the results of the analysis are summarized in Table 1. On the first heating scan, the as-prepared sample of compound **4a** showed a melting (Fig. 1a); upon cooling at a rate of $10^\circ\text{C}/\text{min}$, the compound did not recrystallize but showed a glass transition (Fig. 1g) [26]. On the second heating scan, the compound exhibited a T_g at 82°C without melting (Fig. 1b). Compound **4a** was annealed by heating at the onset of the melting temperature endotherm in order to confirm whether this amorphous property is an intrinsic characteristic. After the annealing, the T_m and T_g were almost unchanged, but the magnitude of melting endotherm was decreased significantly from 32 kJ mol^{-1} to 0.5 kJ mol^{-1} (Fig. 1c). Again, during cooling, the compound would not recrystallize (Fig. 1h). This indicates that compound **4a** only can readily crystallize by precipitation from a non-solvent, whereas once it has

Table 1. Transition temperatures and enthalpy changes of compounds

Compounds	X	DSC Scans	T_g [°C]	aT_c [°C]	$^a\Delta H_c$ [kJ mol ⁻¹]	T_m [°C]	ΔH_m [kJ mol ⁻¹]
4a	H	1st heating cooling 2nd heating	(84) ^b 83 ^c (79) ^b 82(90) ^b			197 ^c (197) ^b	32 ^c (0.5) ^b
4b	<i>o</i> -Cl	1st heating cooling 2nd heating	77 65 74	110	36	215	49
4c	<i>p</i> -Cl	heating cooling		183	43	284	52
4d	CH ₃	heating				165	d
4e	CH ₃ O	heating				162	d
4f	<i>t</i> -Bu	heating				214	d
4g	NO ₂	heating				>250 ^e	

^a T_c and ΔH_c stand for the recrystallization temperature and the associated enthalpy change, respectively. ^bData in parenthesis was obtained after annealing for 12 h at 170°C. ^cThe data of the reference 26 was included for comparison. ^dNot available. ^eMelting coincides with thermal decomposition.

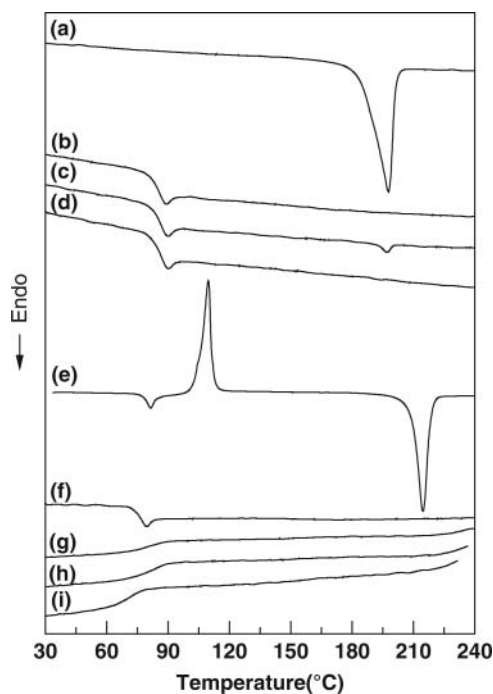


Figure 1. DSC curves of compounds **4a** and **4b** (heating and cooling rates = 10°C/min): **4a** (as-prepared): (a) 1st heating, (b) 2nd heating, and (g) 1st cooling scans; **4a** (annealed at 170°C for 12 h): (c) 1st heating, (d) 2nd heating, and (h) 1st cooling scans; **4b** (as-prepared): (e) 1st heating, (f) 2nd heating, and (i) 1st cooling scans.

Table 2. General properties of polymers

Polymers	Ar	η_{inh} [dL/g]	T_g [°C]	aT_d [°C]	Residue at 600°C [wt%]
7a	<i>m</i> -Ph	0.30 ^b	247	430	65
7b	<i>p</i> -Ph	0.35 ^c	243	420	36

^a T_d stands for the initial decomposition temperature. ^bMeasured using a 0.5 g/dL solution of CHCl_3 at 30°C. ^cMeasured using a 0.5 g/dL solution of H_2SO_4 at 30°C.

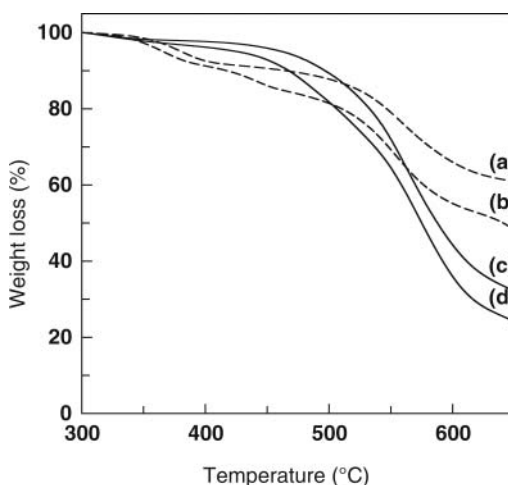


Figure 2. TGA curves of (a) precursor **6a**, (b) precursor **6b**, (c) polymer **7a**, and (d) polymer **7b** (heating rate = 20°C/min).

melted, the compound cannot recrystallize easily in its bulk state. On the first heating scan, the as-prepared sample of compound **4b** exhibited three thermal transitions: a glass transition, crystallization, and melting (Fig. 1e). Similar to **4a**, once it was melted, **4b** would not recrystallize easily (Fig. 1, f and i). An increase in conformational variability due to the *o*-chloro-substitution may account for the unique crystallization behavior of **4b**. In Table 1, the T_g of **4b** is not higher than that of **4a**, indicating that the libration is mainly correlated with reorientation of the entire bent conformation rather than regional steric hindrance due to *o*-substitution by the chlorine atom. Compounds **4c–4f** were normal crystalline compounds with T_m 's in the range of 162–284°C. However, compound **4g** with a nitro group exhibited thermal decomposition at about 250°C after melting.

Table 2 presents the general properties of the polymers. Poly(1,3,4-oxadiazole) with a nonlinear *m*-phenylene unit has better solubility in common organic solvents than that of poly(1,3,4-oxadiazole) with a linear *p*-phenylene unit. The inherent viscosities (η_{inh}) of polymers **7a** and **7b** are 0.30 and 0.35, respectively, indicating that the polymers do not have a very high molecular weight. The polymers have a glass transition temperature (T_g) without melting according to their DSC thermograms, indicating their amorphous nature. Note that even though the value of solution viscosity for polymer **7a** was lower than polymer **7b**, the T_g of the former polymer with the nonlinear *m*-phenylene moiety is higher than the latter polymer with the linear *p*-phenylene moiety. The thermal stability of the polymers in a nitrogen atmosphere was studied by TGA. Fig. 2 shows that the thermal

stability of polymers could be enhanced by cyclodehydration of the hydrazide prepolymers to poly(1,3,4-oxadiazole)s. In Table 2, the decomposition temperatures (T_d) of poly(1,3,4-oxadiazole)s emphasize the good thermal stability of the polymers even those with a highly nonlinear *o*-terphenyl core.

3.2. Absorption and Photoluminescence Properties

The absorption spectra of compounds **4a–4f** in CHCl_3 solution and polymer **7a** are shown in Fig. 3a. The absorption maximums of the compounds span 281–324 nm depending on the substituent, and that of polymer **7a** was 299 nm (see Table 3), substantially red-shifted in comparison with biphenyl (246 nm) and *p*-terphenyl (278 nm) [27]. Considering the fact that the unsubstituted 2,5-diphenyl-1,3,4-oxadiazole (DPO) shows an optical absorption peak at 284 nm [5f], we suggest that a highly extended delocalized system which typically dominates the system's absorption was formed throughout the *o*-terphenyl core. The absorption maxima of compounds **4e** with an electron donor, **4g** with an electron acceptor, and **4d** and **4f** with alkyl groups were observed at 303, 324, 294, and 299 nm, respectively; all were substantially red-shifted in comparison with those of **4a** (286 nm) without substitution, and **4b** (287 nm), **4c** (281 nm) with a Cl-substituent. As can be seen from Fig. 3a, the nitro group exhibits the largest red-shift with the most distinctive shoulder absorption. This can be accounted for the increased band gap due to its electron withdrawing character. On the other hand, polymer **7a** showed an absorption maximum at 295 nm. However, spectra of polymer **7b** could not be measured because of poor solubility in common organic solvents.

The PL spectra of compounds **4a–4f** in CHCl_3 solution, and polymer **7a** are shown in Fig. 3b; three of them show the vibronic feature. The PL maxima of these samples occurred near 398–405 nm (see Table 3), which was substantially red-shifted in comparison with that of DPO (365 nm). As a result, found were the materials emitting light in the violet and indigo region; no emission from compound **4g** with a nitro group was observed when photoexcited, probably due to exciton quenching.

Table 3. Physical properties of compounds and polymers

Sample Code	X or Ar	CHCl ₃ Solution		Film on Glass		
		UV_{\max} [nm]	PL_{\max} [nm]	UV_{\max} [nm]	$^aPL_{\max}$ [nm]	$^bEL_{\max}$ [nm]
4a	H	286	398,447 ^c	d	403,452 ^c (408,456 ^c)	d
4b	<i>o</i> -Cl	287	401,450 ^c	d	401,460 ^c (401)	d
4c	<i>p</i> -Cl	281	398,447 ^c	308	403,446 ^c (403)	451
4d	CH ₃	294	391	269 ^c ,310	408,466 ^c	
4e	CH ₃ O	303	400	308	431	454(440)
4f	<i>t</i> -Bu	299	403	298	410	442
4g	NO ₂	324,278 ^c				
7a	<i>m</i> -Ph	299	405	297	415,464 ^c	

^aData in parenthesis was for crystal samples, while remaining data for glassy samples. ^bData in parenthesis was taken from the device of [ITO/CUPC/compound/LiF: Al], while remaining data from the device of [ITO/ α -NPB/compound/TPBi/Alq₃/LiF/Al]. ^cShoulder peak. ^dNot available.

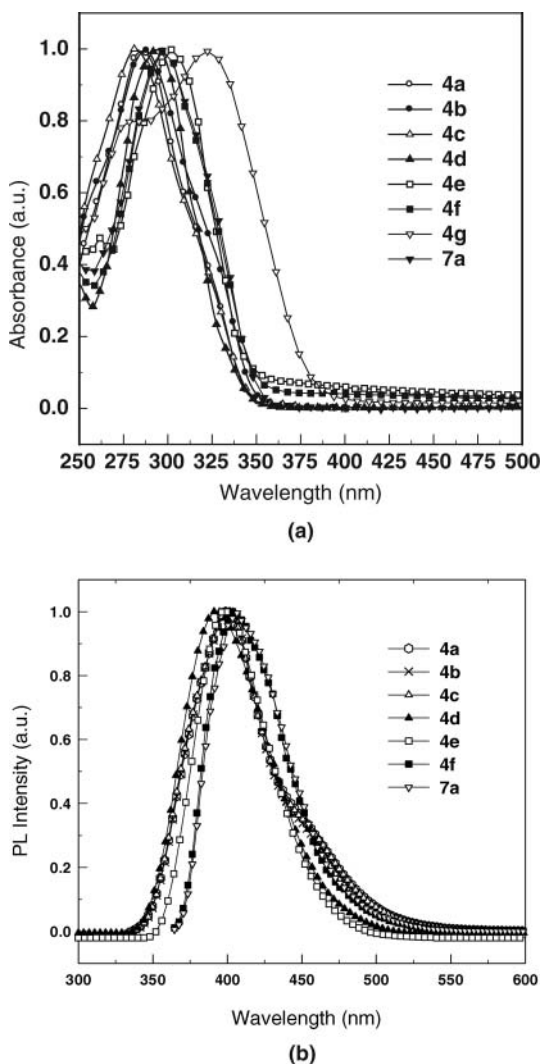


Figure 3. (a) UV-Vis absorption and (b) PL spectra of compounds and a polymer in CHCl_3 solution at room temperature.

The PL spectra of compounds **4a** and **4b** in different physical states are compared in Fig. 4. Glassy samples were prepared by rapidly cooling the melts to room temperature; crystalline samples were prepared by adhering the solid to an indium plate using a glass “rolling pin”. For compound **4a**, the peak wavelength at 398 nm in solution shifted to 403 nm in the glassy state, and to 408 nm in the crystalline state, respectively. These red-shifts imply that the π -orbital overlapping increases because the mobility of conjugated bond remains low in the glassy and the crystalline states with a low degree of crystallinity due to molecular packing constraints of highly bent *o*-terphenyl groups as well as the DPO backbone retaining its rigidity. However, as can be seen in Fig. 4, the spectra of compound **4b** differ insignificantly with the physical state.

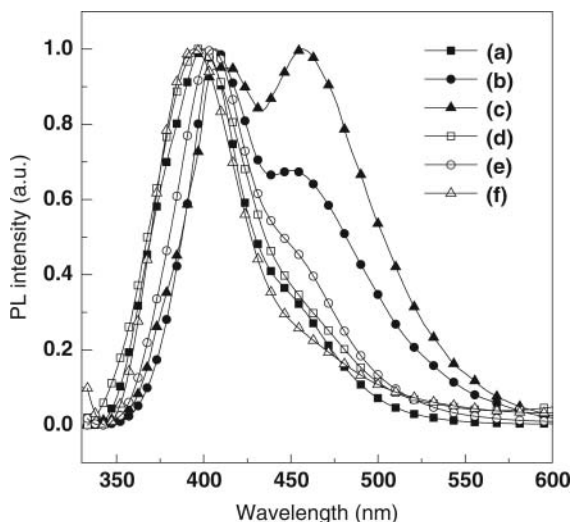


Figure 4. PL spectra of compounds **4a** and **4b** at different physical states: (a) CHCl_3 solution, (b) glassy and (c) crystal samples of **4a**; (d) CHCl_3 solution, (e) glassy and (f) crystal samples of **4b**.

The absorption and emission spectra of the solid state of compounds **4c–4f** and polymer **7a** are shown in Fig. 5. Films on glass were prepared by spin-coating from a CHCl_3 solution. A similar red-shift trend found in solutions was observed and depended on substituents. Generally, due to aggregation in the crystalline states, spectra of samples were substantially red-shifted in comparison with those observed in solutions. The PL maximum of compound **4e** with a methoxy group revealed the highest red-shift of all of the samples, indicating a morphological changes potentially stemming from interactions between the electron accepting 1,3,4-oxadiazole and the electron donating methoxy groups.

3.3. Electroluminescence Properties

The current density versus voltage (J-V) characteristics of the devices based on compounds **4d–4f** and polymer **7a** are compared in Fig. 6a. The EL threshold voltage of the devices with compounds **4d**, **4e** and **4f** was 1.0, 1.3 and 0.8 MV cm^{-1} , respectively. Energy levels of compounds **4c**, **4e** and **4f** from ultraviolet photoelectron spectroscopy (UPS) have been determined: the HOMO energy levels of compounds **4c**, **4e**, and **4f** are 6.08, 6.05 and 5.75 eV, respectively, and the LUMO levels are 2.49, 2.49, and 2.16 eV, respectively. The band energy diagrams of the devices with different materials and structures are compared in Fig. 7. It is expected that hole injection from the anode to compound **4f** will be more favorable than to compound **4e**. Therefore the current density of the devices with compounds **4d** and **4f** with an alkyl group is higher than that of compound **4e** with an alkoxy group as shown in Fig. 6a. As a result, the driving voltage required to obtain the same current density is lower for compounds **4d** and **4f** than for compound **4e**. However, a high current density does not necessarily guarantee a high quantum efficiency of the EL device, especially when the hole current prevails over the electron current leading to largely unbalanced charge carrier injection. The device with compound **4e** can give a higher quantum efficiency than those with compounds **4d** and **4f** if hole and electron injection is better balanced at the same current density (see Fig. 6b). In addition, compound **4e** has an intramolecular

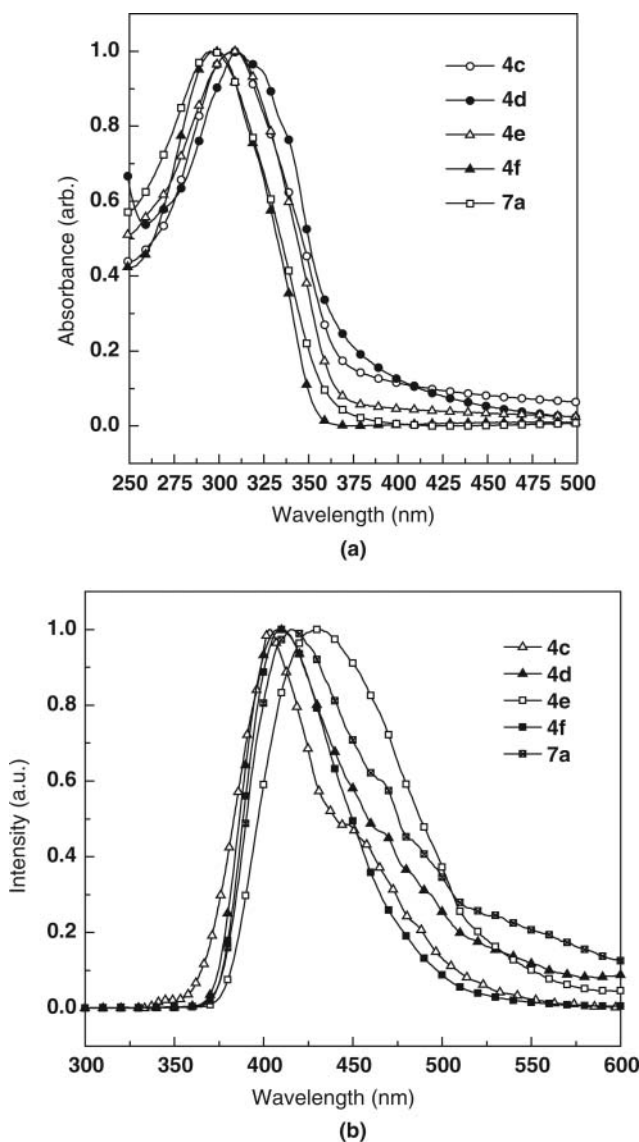


Figure 5. (a) UV-Vis absorption and (b) PL spectra of compounds and a polymer in solid state at room temperature.

charge-transfer complex between the electron-withdrawing 1,3,4-oxadiazole moiety and the electron-releasing 4-methoxy-phenyl moiety. It is probable that the intramolecular donor-acceptor (D-A) type complex formed in compound **4e** can trap holes as well as electrons more efficiently than compounds **4d** and **4f**. Therefore, we can suggest that compound **4e** is the best deep blue light-emitting material among the compounds in spite of having the highest driving threshold voltage.

In Fig. 8, the EL spectra of the devices with compounds **4c**, **4e** and **4f** show deep-blue EL emissions with a peak at 440–454 nm (see Table 3). The general appearance of the EL spectra of these compounds was relatively red-shifted in comparison with the PL spectra

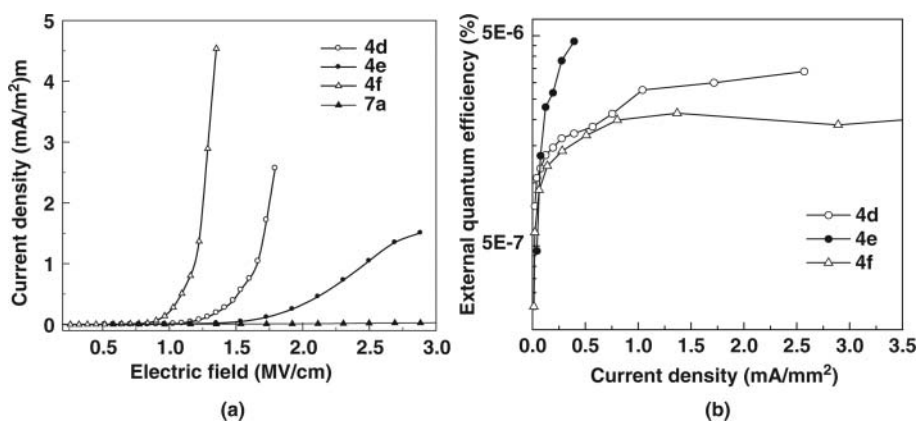


Figure 6. (a) Current density on applied electric field strength in EL devices of [ITO/CUPC/4d–4f/LiF:Al] and [ITO/PEDOT/7a/LiF:Al]. (b) External quantum efficiencies on applied electric field strength in EL device of [ITO/CUPC/4d–4f /LiF:Al].

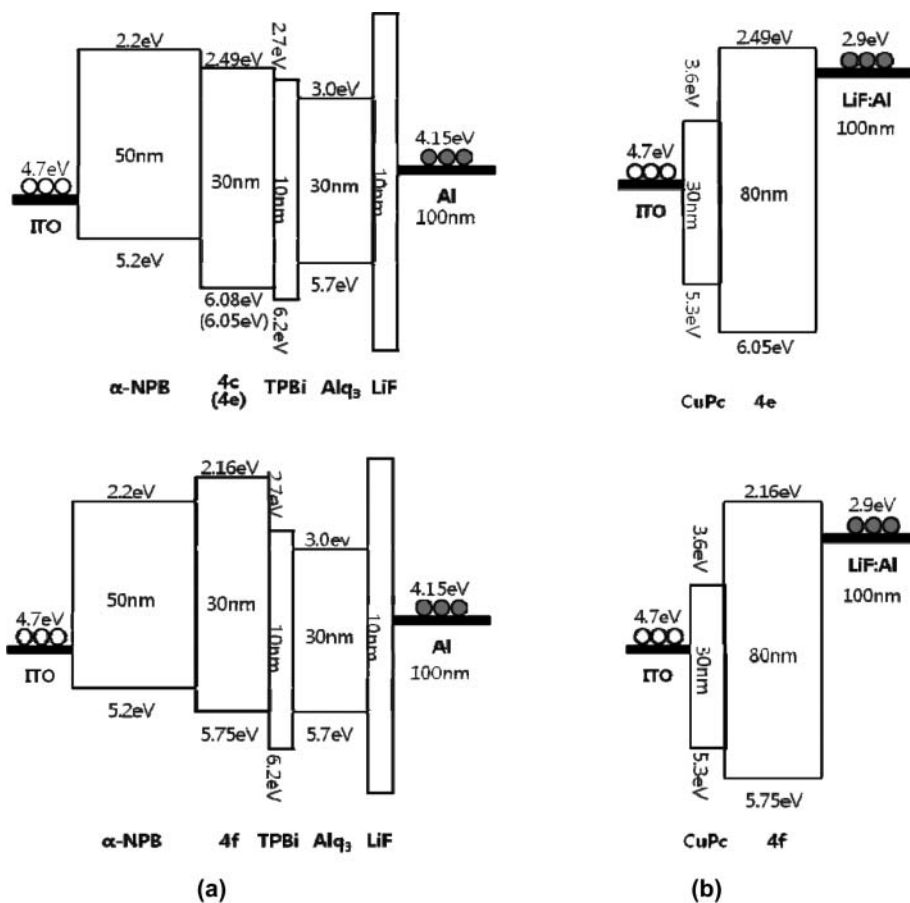


Figure 7. Schematic energy band diagrams of the energy band for two different devices: (a) [ITO/α-NPB/4c, 4e and 4f/TPBi/Alq₃/LiF/Al]; (b) [ITO/CUPC/4e and 4f/LiF:Al].

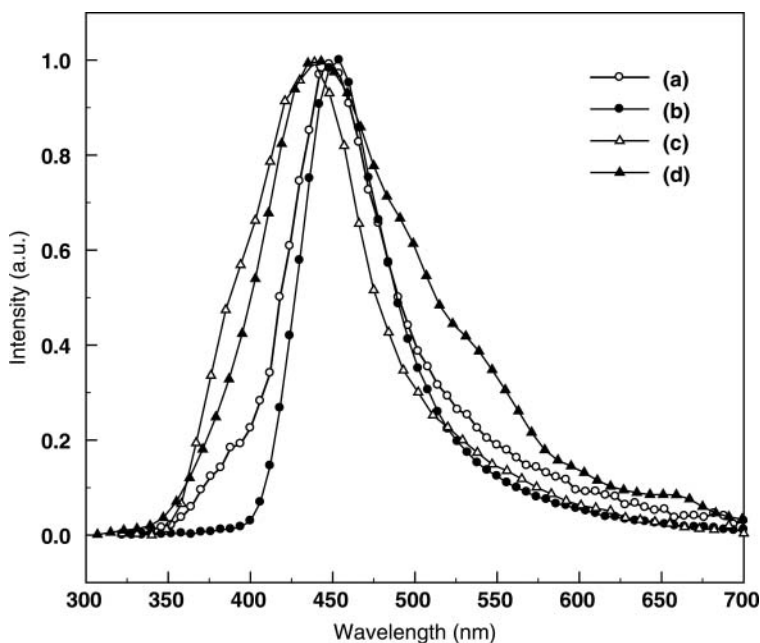


Figure 8. EL spectra of the devices with compounds **4c**, **4e** and **4f**: [ITO/ α -NPB/(a) **4c**, (b) **4e** or (c) **4f** /TPBi/Alq₃/LiF/Al] and [ITO/CUPC/(d) **4e**/LiF/Al].

in solid state. Previously, it was reported that the second substituent in DPO influences the emission wavelength: using an electron donor, the material emits in the blue; with an electron acceptor in the green spectral range [18f]. However, compound **4g** with a nitro group does not luminescence at all. Compound **4e** showed a different EL maximum depending on the configuration of the EL device, maintaining the blue-light-emitting property. The deep blue OLED device using **4c**, **4e**, and **4f** as an EML has a maximum luminance of 240, 1120 and 220 cd/m², respectively. The CIE coordinates of compounds **4c**, **4e**, and **4f** in the EL devices with the configuration of [ITO/ α -NPB/compound/TPBi/Alq₃/LiF/Al] were found to be (0.19, 0.16), (0.17, 0.13) and (0.18, 0.13), respectively, i.e., in the deep-blue region.

4. Conclusions

A series of *o*-terphenyl-1,3,4-oxadiazole derivatives and two poly(*o*-terphenyl-1,3,4-oxadiazole)s were synthesized by a dehydration reaction of hydrazide precursors. The *o*-chloro- and unsubstituted compounds form glasses with a *T*_g in the range of 65–90°C depending on the thermal history: The PL spectrum of the unsubstituted compound in a glass is closer to the spectrum in solution than in the crystal. The absorption and the PL maximums of compounds with a substituent such as methyl, methoxy, and *t*-butyl groups were substantially red-shifted in comparison to those of compounds with *o*-chloro- and *p*-chloro-substituents or without a substituent. The absorption maximum of the compound with a nitro group exhibited the largest red-shift, but this compound did not emit light after electrical excitation nor photoexcitation. The absorption and PL maxima of the *m*-phenylene-based polymer were red-shifted in comparison with the compounds, which emitted indigo-light ($\lambda_{\text{PL,max}} = 415$ nm). Moreover, EL maxima of compounds with methyl,

methoxy and t-butyl groups were found at deep-blue-light region ($\lambda_{\text{EL,max}} = 440\text{--}454\text{ nm}$). According to thermal analysis, the two polymers possess amorphous characteristics as well as good thermal stability. Moreover, the *m*-phenylene-based polymer revealed good solubility in general organic solvents and emits indigo-light at 415 nm on photoexcitation.

Acknowledgement

This work was supported by Grant No. R01-2005-000-10852-0, from the Basic Research Program of the Korean Science & Engineering Foundation and in part by NSF Grant DMR-9971143.

References

- [1] Tang, C., VanSlyke, S. (1987). *Appl. Phys. Lett.*, **51**, 913–915.
- [2] Tetsuya, N., Hiromitsu, O., Yasuhiko, S. (1999). *Adv. Mater.*, **11**, 283–285.
- [3] Kido, J., Lizumi, Y. (1998). *Appl. Phys. Lett.*, **73**, 2721–2723.
- [4] Shi, J., Tang, C. (2002). *Appl. Phys. Lett.*, **80**, 3201–3203.
- [5] Liao, C., Lee, M., Tsai, C., Chen, C. (2005). *Appl. Phys. Lett.*, **86**, 203507–203509.
- [6] Wu, Y., Zheng, X., Zhu, W., Sun, R., Jiang, X., Zhang, Z., Xu, S. (2003). *Appl. Phys. Lett.*, **83**, 5077–5079.
- [7] Meng, H., Herron, N. In: Li, Z., Meng, H. editors. “*Organic Light-Emitting Materials and Devices*”, New York: Taylor & Francis Group, (2007). pp. 295–412.
- [8] Park, Y.-I., Son, J.-H., Kang, J.-S., Kim, S.-K., Lee, J.-H., Park, J.-W. (2008). *Chem. Commun.*, **18**, 2143–2145.
- [9] Fang, Z., Wang, S., Zhao, L., Xu, Z., Ren, J., Wang, X., Yang, Q. (2008). *Mater. Chem. Phys.*, **107**, 305–309.
- [10] He, Q., Chu, Z., Lei, G., Qin, A., Lin, H., Bai, F., Cheng, J., Qiu, Y. (2008). *Chin. Chem. Lett.*, **19**, 431–434.
- [11] Zhu, Y., Gibbons, K., Kulkarni, A., Jenekhe, S. (2007). *Macromolecules.*, **40**, 804–813.
- [12] Li, Z., Xiong, M., Wong, M. (2007). *Chin. Chem. Lett.*, **18**, 823–826.
- [13] Koguchi, R., Kobayashi, N., Shinnai, T., Oikawa, K., Tsuchiya, K., Kijima, M. (2008). *Macromol. Chem. Phys.*, **209**, 439–449.
- [14] Lai, W., Zhu, R., Fan, Q., Hou, L., Cao, Y., Huang, W. (2006). *Macromolecules.*, **39**, 3707–3709.
- [15] Shen, Q., Ye, S., Yu, G., Lu, P., Liu, Y. (2008). *Synth. Met.*, **158**, 1054–1058.
- [16] Zhang, W., Jin, W., Zhou, X., Pei, J. (2007). *Tetrahedron Lett.*, **63**, 2907–2914.
- [17] (a) Schulz, B., Knochenhauer, G., Brehmer, L., Janietz, J. (1995). *Synth. Met.*, **69**, 603–604. (b) Pommerehne, J., Vestweber, H., Guss, W., Mahrt, R., Bässler, H., Porsch, M., Daub, J. (1995). *Adv. Mater.*, **7**, 551–554. (c) Pei, Q., Yang, Y. (1995). *Chem. Mater.*, **7**, 1568–1575. (d) Thünemann, A., Janiez, S., Anlauf, S., Wedel, A. (2000). *J. Mater. Chem.*, **10**, 2652–2656. (e) Murata, H. (2001). *Synth. Met.*, **121**, 1679–1680; Schulz, B., Bruma, M., Brehmer, L. (1997). *Adv. Mater.*, **9**, 601–613.
- [18] (a) Yang, Y., Pei, Q. (1995). *J. Appl. Phys.*, **77**, 4807–4809. (b) Buchwald, E., Meier, M., Karg, S., Pösch, P., Schmidt, H., Strohmriegl, P., Riess, W., Schwoerer, M. (1995). *Adv. Mater.*, **7**, 839–842. (c) Meier, M., Buchwald, E., Karg, S., Pösch, P., Greczmiel, M., Strohmriegl, P., Riess, W. (1996). *Synth. Met.*, **76**, 95–99. (d) Janietz, S., Wedel, A., Friedrich, R. (1997). *Synth. Met.*, **84**, 381–382; Schulz, B., Kaminorz, Y., Brehmer, L. (1997). *Synth. Met.*, **84**, 449–450. (e) Kaminorz, Y., Schulz, B., Schrader, S., Brehmer, L. (2001). *Synth. Met.*, **122**, 115–118. (f) Janietz, S., Anlauf, S. (2002). *Macromol. Chem. Phys.*, **203**, 427–432. (g) Janietz, S., Anlauf, S., Wedel, A. (2002). *Macromol. Chem. Phys.*, **203**, 433–438.
- [19] Mitschke, U., Bäuerle, P. (2000). *J. Mater. Chem.*, **10**, 1471–1507.
- [20] Kraft, A., Grimsdale, A., Holmes, A. (1998). *Angew. Chem. Int. Ed.*, **37**, 402–428.

- [21] (a) Tang, C., VanSlyke, S. (1998). *Appl. Phys. Lett.*, **51**, 913–915. (b) Adachi, C., Tokito, S., Tsutsui, T., Saito, S. (1988). *Jpn. J. Appl. Phys.*, **27**, L269–271.
- [22] (a) Bettenhausen, J., Strohriegl, P., Brütting, W., Tokuhisa, H., Tsutsui, T. (1997). *J. Appl. Phys.*, **82**, 4957–4961. (b) Tokito, S., Tanaka, H., Noda, K., Okada, A., Taga, Y. (1997). *Macromol. Symp.*, **125**, 181–185.
- [23] (a) Bettenhausen, J., Strohriegl, P. (1996). *Adv. Mater.*, **8**, 507–510. (b) Bettenhausen, J., Strohriegl, P. (1996). *Macromol. Rapid Commun.*, **17**, 623–631.
- [24] Kraft, A. (1996). *Chem. Commun.*, 77–79.
- [25] Shi, J., Tang, C., Chen, C. (1997). *U.S. Patent 5645948*.
- [26] Zafiropoulos, N., Choi, E.-J., Dingemans, T., Lin, W., Samulski, E. (2008). *Chem. Mater.*, **20**, 3821–3831.
- [27] (a) Berlman, I., Wirth, H., Steingraber, O. (1971). *J. Phys. Chem.*, **75**, 318–325. (b) Nijegorodova, N., Downey, W., Danailov, M. (2000). *Spectrochim. Acta Part A*, **56**, 783–795.